mathematics

MDPI

Article

Using Value-Based Potentials for Making Approximate Inference on Probabilistic Graphical Models

Pedro Bonilla-Nadal †, Andrés Cano †, Manuel Gómez-Olmedo *,†, Serafín Moral † and Ofelia Paula Retamero †

Computer Science and Artificial Intelligent Department, University of Granada, 18071 Granada, Spain; pedrobn@ugr.es (P.B-N.); acu@decsai.ugr.es (A.C.); smc@decsai.ugr.es (S.M.); oretamero@decsai.ugr.es (O.P.R.)
* Correspondence: mgomez@decsai.ugr.es; Tel.: +34-958248487
† These authors contributed equally to this work.

Abstract: The computerization of many everyday tasks generates vast amounts of data, and this has lead to the development of machine-learning methods which are capable of extracting useful information from the data so that the data can be used in future decision-making processes. For a long time now, a number of fields, such as medicine (and all healthcare-related areas) and education, have been particularly interested in obtaining relevant information from this stored data. This interest has resulted in the need to deal with increasingly complex problems which involve many different variables with a high degree of interdependency. This produces models (and in our case probabilistic graphical models) that are difficult to handle and that require very efficient techniques to store and use the information that quantifies the relationships between the problem variables. It has therefore been necessary to develop efficient structures, such as probability trees or value-based potentials, to represent the information. Even so, there are problems that must be treated using approximation since this is the only way that results can be obtained, despite the corresponding loss of information. The aim of this article is to show how the approximation can be performed with value-based potentials. Our experimental work is based on checking the behavior of this approximation technique on several *Bayesian networks* related to medical problems, and our experiments show that in some cases there are notable savings in memory space with limited information loss.

Keywords: probabilistic graphical models; bayesian networks; value-based potentials; approximate inference; medical applications

MSC: 68T37; 62C10; 62F15

Citation: Bonilla-Nadal, P.; Cano, A.; Gómez-Olmedo, M.; Moral, S.; Retamero, O.P. Using Value-Based Potentials for Making Approximate Inference on Probabilistic Graphical Models. *Mathematics* **2022**, *10*, 2542. https://doi.org/10.3390/math10142542

Academic Editors: Carmen Lacave and Ana Isabel Molina

Received: 13 June 2022
Accepted: 14 July 2022
Published: 21 July 2022

1. Introduction

Probabilistic Graphical Models (*PGMs*) [1–3] are a powerful framework to encode problems under uncertainty. *PGMs* are able to combine graphs and probability theory to compactly represent the probabilistic dependency between random variables. Any *PGM* can be defined by its two components:

- Qualitative component, given by a directed, acyclic graph (*DAG*), where each node represents a random variable, and the presence of an edge connecting two of these implies mutual dependency.
- Quantitative component, given by a set of parameters that quantify the degree of dependence between the variables.

One of the most interesting properties of *PGMs* over discrete domains such as *Bayesian networks* (*BNs*) [4,5] and *influence diagrams* (*IDs*) [6,7] is the efficient representation of joint probability distributions, and traditionally marginal or conditional probability distributions and utility functions are represented with *tables* or *unidimensional arrays* (*1DA* in general). However, as the size of *1DAs* grows exponentially with the number of variables, an exact

representation might be arduous or even impossible (due to memory space restrictions). Even in cases where problem representation using *1DA* is possible, it may be difficult to perform subsequent inference tasks as new potentials may appear larger than the initial ones.

This difficulty originates some works focused on improving the way of performing operations with probability distribution and utility functions as a way to alleviate the computational cost in complex models [8]. And another approaches have been explored over the years in the search for efficient alternative representations to *1DAs*, which are able to work with complex models. Successful examples are standard and binary probability trees (*PTs* and *BPTs*) [9–13]. Despite the advantages that these offer compared to the use of *1DA*, they also present certain limitations, and not all context-specific independences can result in smaller representations and therefore in memory space savings.

Another very well-studied strategy for saving memory space is to approximate the structures, such as in *PTs*, by accepting a loss of information [14,15]. This operation is called pruning and the *PTs* which have been pruned are called *pruned probability trees* (*PPTs*). This operation consists of replacing certain contiguous values with their average value, always remembering to select those values that produce the smallest information loss.

Value-based potentials (*VBPs*) [16] were recently introduced. These structures take advantage of the repetition of values, regardless of the order in which they appear. *VBPs* were tested with several *BNs* included in the *bnlearn* repository [17,18] and the *UAI* inference competitions [19,20]. The paper compares the memory spaces required for representing potentials with *1DAs*, *PTs*, *PPTs*, and *VBPs*. The comparison demonstrates that there is an overall reduction in memory space when *VBPs* are used. Their use is justified by observing that, in a large number of *BNs* representing real-world problems (in the medical field, for example), many repeated values appear in the potentials which quantify the probabilistic relationships. For example, all those impossible events will have been assigned a probability value equal to 0. Another source of repetition can occur in situations in which the models include subjectively assigned probabilities through interviews with experts. Normally, the assigned probabilities are reduced to a very limited set of values (for example, 0.25, 0.4, etc., and it is difficult for an expert to indicate that the probability of an event occurring is 0.23678).

Taking into account all of the previously mentioned work, the aim of our study will be to make *VBPs* even more compact and to define an algorithm to approximate them. Such an algorithm will be an iterative process, and each step will keep the approximated *VBP* with the minimum Kullback–Leibler divergence in relation to the original one, thereby minimizing loss of information.

This paper is organized as follows: Section 2 defines some necessary basic concepts and notation; Section 3 contains the theory about classical structures and alternative *VBPs*; Section 4 introduces the prerequisites for the approximation of *VBPs* and the approximation algorithm itself; Section 5 studies the empirical evaluation of the algorithm by applying it to real *BNs*; and finally Section 6 outlines our conclusions and presents our future lines of research.

2. Basic Definitions and Notation

Let $\mathbf{X} = \{X_1, X_2, \ldots, X_N\}$ be a finite set of discrete random variables. For the sake of simplicity, the states of each variable X_i (its *domain*) are assumed to be integers and represented as Ω_{X_i}. The values for X_i are noted in lowercase $\Omega_{X_i} = \{x_{i,j} \ : \ j = 1, 2, \ldots, k_i\}$. $|\Omega_{X_i}|$ denotes the *cardinality* of the variable, i.e., the number of elements in its domain ($|\Omega_{X_i}| = k_i$).

The Cartesian product $\prod_{X_i \in \mathbf{X}} \Omega_{X_i}$ will be denoted as $\Omega_{\mathbf{X}}$ and its elements, called *configurations* of $\mathbf{X}$, are defined by $\mathbf{x} := \{X_1 = x_1, X_2 = x_2, \ldots, X_N = x_n\}$, or $\mathbf{x} := \{x_1, x_2, \ldots, x_n\}$ (if the variables are obvious from the context). A function defined over a subset of variables $\mathbf{Y} \subseteq \mathbf{X}$ and taking values in $\mathbb{R}_0^+$ will be termed as a *potential* $\phi(\mathbf{Y})$.

Example 1. *Let us consider the variables X_1, X_2, and X_3, with 2, 3, and 2 possible states, respectively. Then $\phi(X_1, X_2, X_3)$ is a potential defined on such variables with the values assigned to each configuration shown in Figure 1. This potential expresses the conditional distribution $P(X_3|X_1, X_2)$.*

index	x_1	x_2	x_3	$\phi(x_1, x_2, x_3)$
0	0	0	0	0.1
1	0	0	1	0.9
2	0	1	0	0.5
3	0	1	1	0.5
4	0	2	0	0.0
5	0	2	1	1
6	1	0	0	0.8
7	1	0	1	0.2
8	1	1	0	0.2
9	1	1	1	0.8
10	1	2	0	0.9
11	1	2	1	0.1

Figure 1. Representation of the potential $\phi(X_1, X_2, X_3)$ as a mapping that assigns a numeric value to each configuration.

In order for some of the structures considered in our work to be better understood, we need to clarify the concept of the *index of configuration*. This is a unique, numeric identifier which represents each configuration on a given domain $\Omega_{\mathbf{X}}$. Let us consider that the indices start at 0 and end on $|\Omega_{\mathbf{X}}| - 1$. In the given Example 1, *index 0* is associated with the configuration $\{0, 0, 0\}$, *index 1* to $\{0, 0, 1\}$, and so on until the last one, *11*, which is associated with $\{1, 2, 1\}$ (these indices are shown in the left-most column in Figure 1).

There is a relation between indices and configurations based on the concept of *weight* (otherwise known as *stride* or *step size*). Assuming an order between variables $\mathbf{X} = \{X_1 \dots X_N\}$, each variable $X_i \in \mathbf{X}$ has an associated weight w_i that may be computed as follows (variable with index N has the lowest weight):

$$w_i = \begin{cases} 1 & if \quad i = N \\ |\Omega_{X_{i+1}}| \cdot w_{i+1} & otherwise. \end{cases} \tag{1}$$

The index corresponding to a certain configuration $\mathbf{x} = \{x_1, x_2, \dots, x_N\}$ can be computed as:

$$index(\mathbf{x}) = \prod_{i=1}^{N} x_i \cdot w_i. \tag{2}$$

Example 2. *Considering the potential described in Example 1, the weights are $w_3 = 1, w_2 = 2, w_1 = 6$, and the indices assigned to configurations are presented below:*

$$\begin{aligned} index(\{0,0,0\}) &= 0 \cdot 6 + 0 \cdot 2 + 0 \cdot 1 = 0 \\ index(\{0,0,1\}) &= 0 \cdot 6 + 0 \cdot 2 + 1 \cdot 1 = 1 \\ index(\{0,1,0\}) &= 0 \cdot 6 + 1 \cdot 2 + 0 \cdot 1 = 2 \\ &\dots\dots\dots\dots \\ index(\{1,2,1\}) &= 1 \cdot 6 + 2 \cdot 2 + 1 \cdot 1 = 11 \end{aligned}$$

More specifically, the value of a particular variable X_i in a configuration linked to an index k, denoted by $\mathbf{x}^{(k)}$ and satisfying $index(\mathbf{x}^{(k)}) = k$, can be computed as:

$$x_i = (k//w_i) \,\%\, |\Omega_{X_i}|, \tag{3}$$

where // denotes integer division and % the modulus of the division.

As we mentioned previously, the association between indices and configurations requires that the variable order in the domain be known. Any order is valid, but by default, we will consider the order in which variables are written (e.g., for potential $\phi(X, Y, Z)$, the first variable would be X). Additionally, we consider that the first variable has the highest weight. However, the opposite approach could also be considered.

The links in the network define a set of conditional dependences and independences that are expressed as $X \perp_{\mathbf{Z}} Y$. This expression indicates that X is independent of Y once the values of the variables in $\mathbf{Z}$ are known. The *Markov blanket* of X, $mb(X)$, contains its parents $pa(X)$, its children $ch(X)$, and the parents of the children $pa(ch(X))$; it is the set of variables that makes X be independent of the other variables $\mathbf{Z}$, $\mathbf{Z} = \mathbf{X} \setminus \{X \cup mb(X)\}$, once the value of variables in $mb(X)$ is known, i.e., $X \perp_{mb(X)} \mathbf{Z}$. The *in-degree* of X is the number of parents $|pa(X)|$, and the *out-degree* is the number of children $|ch(X)|$. The *average degree* considers the values of *in-degree* and *out-degree*. These values are used to characterize the *BNs* used for experiments (see details in Table 5).

3. Representation of Potentials

3.1. Classic Structures

3.1.1. 1D-Arrays

A *one-dimensional* or *single-dimensional array* (*1DA*) is a storage structure for elements of the same nature, which enables every element to be accessed individually by specifying the index corresponding to the position where it is located.

Let ϕ be a potential defined over a set of N variables, ϕ can be represented by an *array* $\mathcal{A}_\phi$ as:

$$\mathcal{A}_\phi := \Big[\phi(0,\dots 0), \phi(0,\dots 1), \dots, \phi(|\Omega_{X_1}|-1,\dots,|\Omega_{X_N}|-1)\Big]. \tag{4}$$

The size of a *1DA*, denoted by $size(\mathcal{A}_\phi)$, is the number of entries, or the number of configurations of the potential.

Example 3. *The potential $\phi(X_1, X_2, X_3)$ given in Example 1 can be represented as the following 1DA with 12 entries (see Figure 2).*

0	1	2	3	4	5	6	7	8	9	10	11
0.1	0.9	0.5	0.5	0.0	1.0	0.8	0.2	0.2	0.8	0.9	0.1

Figure 2. $\phi(X_1, X_2, X_3)$ as *1DA*.

3.1.2. Probability Trees

A *probability tree* (*PT*) represents a given potential $\phi : \Omega_{\mathbf{X}} \to \mathbb{R}_0^+$, and allows exact or approximate operations over it [11–13]. A *probability tree* $\mathcal{T}$ is a directed and labeled tree, where each internal node represents one variable and each leaf node a non-negative real number. Each internal node will have as many exiting arcs as the number of states that the variable labeling the node has. The size of a *PT*, $size(\mathcal{T})$, is defined as the number of nodes it contains.

Example 4. *The same potential given in the previous example is presented in Figure 3 as a PT. This PT has 21 nodes (12 leaves and 9 internal nodes).*

PTs can take advantage of context-specific independences [9] by combing equal values into a single one. This operation is called pruning, and once *PTs* have been pruned, they are known as *pruned probability trees* (*PPTs*).

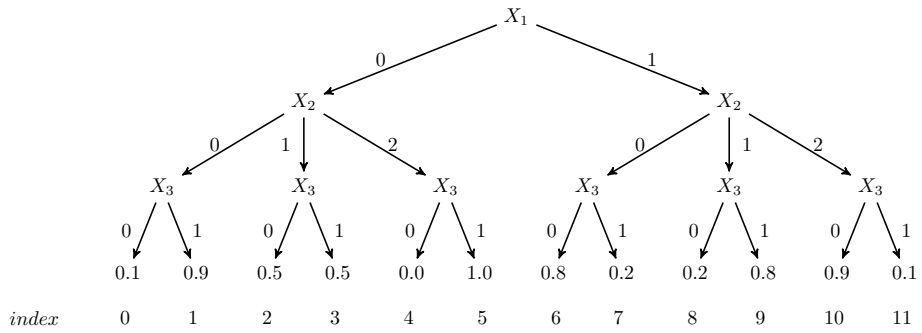

Figure 3. $\phi(X_1, X_2, X_3)$ as *PT*.

Example 5. *The potential in the previous examples presents a context-specific independence that enables its size to be reduced: the value for* $X_1 = 0, X_2 = 1$ *is* 0.5*, regardless of the value of* X_3*. Once the pruning is complete, the result is a PPT consisting of 19 nodes (11 leaves and 8 internal nodes) and this is shown in Figure 4.*

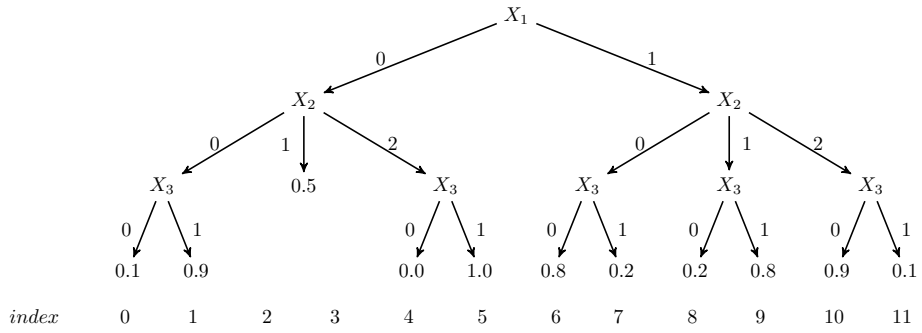

Figure 4. $\phi(X_1, X_2, X_3)$ as *PPT*.

A variant to a *PT* is the *binary probability tree* or *BPT* ([10,14,15]). In *BPTs*, two arcs exit from each internal node, so one variable can label several nodes in a path from root to leaf node. An example of *BPT* is presented in Figure 5 and described in the following example.

Example 6. *On the left, a given PT is represented, and two equal values* (0.4) *can be observed for c configuration (left sub-tree) but related to two different values of* X_k*. Both values can therefore be combined to produce the BPT on the right-hand side of Figure 5. It is now apparent that the leftmost branch of* X_k *simultaneously represents values for* $X_k = 0$ *and* $X_k = 2$*.*

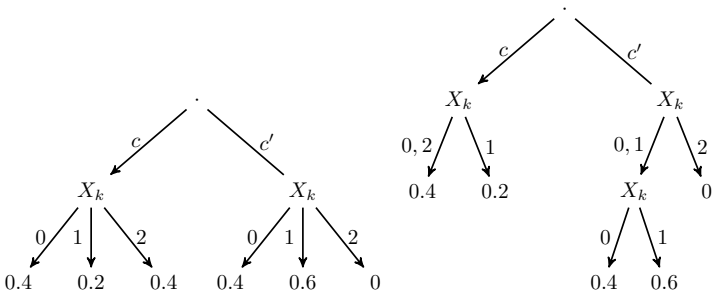

Figure 5. Binary tree representation.

With this property, although *BPTs* can avoid more repetitions of values than *PPTs*, there are still situations in which repetitions cannot be avoided. This is the case for the values 0.4 of the configurations given by c', $x_k = 2$ and c, $x_k = 0$. Therefore, as we mentioned previously, both *PPTs* and *BPTs* introduce the possibility of saving memory space by combining values under pretty specific circumstances, but are not able to make the structure more efficient otherwise. This fact opens various possible avenues of research into how to exploit different

patterns. In many cases, some combinations of values are not allowed and are represented by 0's or some values are repeated several times; a proper efficient structure should be able to somehow compact the information using such patterns.

3.2. Alternative Structures: Value-Based Potentials

Valued-based potentials were recently introduced [16] as an alternative representation based exclusively on the values. Once such new structure was applied on several *BNs* from two different sources (*bnlearn* repository [17,18] and *UAI* competitions [19,20]) and compared with *1DAs*, *PTs*, and *PPTs*. It has been proven that the use of *VBP* structures saves memory space. In *VBPs*, values must be stored paired with the indices (or configurations) that define the events in which they appear. How these pairs value-indices are stored determines two different *VBP* categories:

- Structures driven by values, using dictionaries in which the keys will be values: *value-driven with grains* (*VDG*) and *value-driven with indices* (*VDI*).
- Structures driven by indices, where keys are indices: *index-driven with pair of arrays* (*IDP*) and *index-driven with map* (*IDM*).

In all of these alternatives, a default value is set (in our case, 0.0) and any related index will not be stored (in order to reduce memory space). Such a default value can be defined in advance or may be conveniently selected as the most repeated one. As *VBPs* represent potentials, it will be easy to adapt inference algorithms to use *VBPs*. A more complete definition of *VBPs* can be found in [16].

A simple visual idea of how *VBPs* work can be presented as a set of conveniently arranged probability values (i.e., each value is stored near its corresponding indices). Our studied example will appear as in Figure 6. It should be observed that the index 4, relating to value 0.0 (the default value), is not stored at all. This would be similar to storing the values using a *1DA* structure. However, the goal is to avoid storing duplicated values. The example shows how each of the values, 0.1, 0.2, 0.5, 0.8, and 0.9, appear to be associated with two different indices (or configurations).

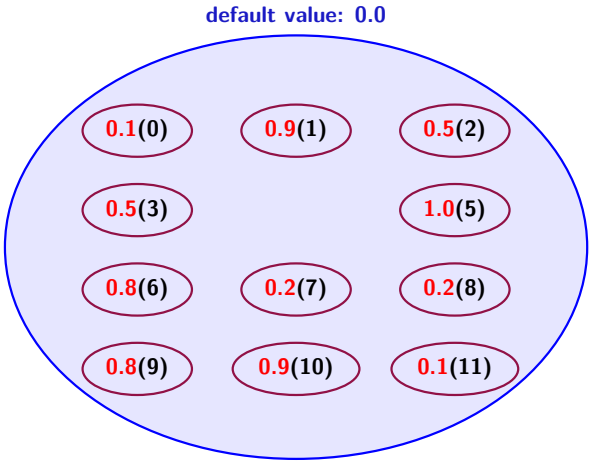

Figure 6. $\phi(X_1, X_2, X_3)$ as the relation between values and indices.

By using *VBPs*, therefore, each value is represented only once and all the indices in which it appears are linked to it. Figure 7 shows the groupings made and this highlights the fact that only 6 probability values are stored. The purpose of *VBPs* is therefore to make as many groups as different probability values exist to avoid repetitions and associate the related indices of configurations.

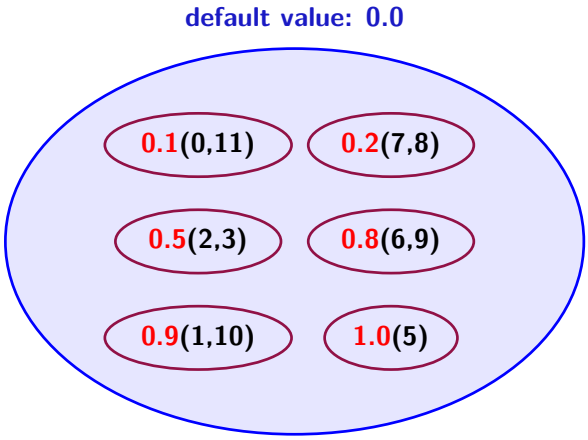

Figure 7. Visual idea of $\phi(X_1, X_2, X_3)$ as grouping equal probability values.

From the alternatives presented in [16], in this paper we will focus on *value-driven with indices* (*VDI*) and *index-driven with pairs* (*IDP*), since both of these performed extremely well on most of the studied *BNs*.

3.2.1. VDI: Value-Driven with Indices

Let us consider a certain potential ϕ defined over $\mathbf{X}$. A *VDI* for ϕ, VDI_ϕ, is a dictionary D in which each entry $< v, L_v >$ contains a value (as the key) and a list of indices L_v, such that $\phi(l) = v$, for each $l \in L_v$.

Example 7. *The potential $\phi(X_1, X_2, X_3)$ used before and described in Figure 1 will be represented as VDI as shown in Figure 8. The outermost rectangle represents the dictionary and the entry keys (values) are drawn as circles. Keys give access to the index lists (inner rectangles with rounded corners). It can be seen that this dictionary faithfully represents the grouping of values shown in Figure 7 as an intuitive explanation of the purpose of VBP structures.*

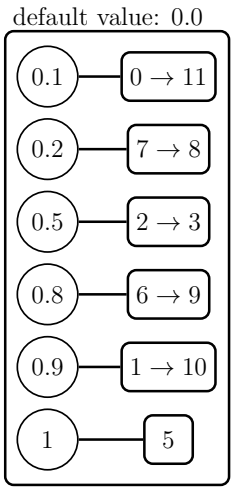

Figure 8. $\phi(X_1, X_2, X_3)$ as *VDI*.

3.2.2. IDP: Index-Driven with Pair of Arrays

Let ϕ be a potential defined over $\mathbf{X}$. A structure *IDP* representing ϕ, IPD_ϕ, is a pair of arrays V and L. Non-repeated values in ϕ (excluding the default value) are stored in $V = \{v_0 \dots v_{d-1}\}$. Let nd_ϕ represent the number of indices storing non-default values. The array L is then defined as follows:

$$L := \{(i, j) : \phi(\mathbf{x}_i) = v_j, i \in nd_\phi\}. \quad (5)$$

This means that *IDP* is based on two components: firstly, an array storing the values (without repetitions and excluding 0.0 as the default value), and secondly, an array of pairs (index in potential, index in array of values). The second index of the pair saves the relationship between the indices and values.

Example 8. *The representation of potential $\phi(X_1, X_2, X_3)$ as IDP is presented in Figure 9. The upper array (V) stores non-default values. The lower one includes pairs of indices. The fourth one $(3, 2)$ represents the fact that $\phi(\mathbf{x}_3) = V(2) = 0.5$.*

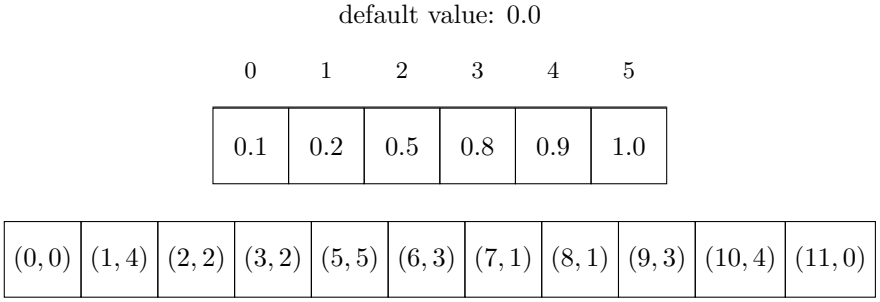

Figure 9. $\phi(X_1, X_2, X_3)$ as *IDP*.

4. Approximating Value-Based Potentials

As we previously mentioned in Section 3, *tables* or *1DA* were widely used in the bibliography to represent quantitative information in *BNs* or *IDs*. There is, however, a limitation of representing potentials with the 1DA structure and that is that they increase exponentially in size as the number of variables increases. Inferring or even dealing with these may therefore be (in the case of complex models) computationally unfeasible. For this purpose, it is convenient not only to define new structures which are able to compactly represent such potentials, but also methods to approximate them so that the memory space may be reduced without any significant loss of information. *PTs* can take advantage of context-specific independences, thereby reducing the number of stored values, but can also be approximated and so produce *PPTs* (this feature was presented as an additional advantage of *PTs* from their definition). However, the guiding procedure for the approach is computationally very expensive as it is necessary to determine the degree of information of each variable in order to ensure that the most informative ones appear as close as possible to the root. This ensures that the values stored in the tree leaves are most similar and, therefore, the loss of information is less when various values are replaced with their average value.

VBP structures [16] may produce a relevant decrease in the memory space when repeated values are present. Moreover, the approximation operation can be applied in a very simple way. This work presents an algorithm for this operation and also provides a theoretical justification for it. Our experimental work will show the performance of the algorithm using two different alternatives for *VBPs*: *value-driven with indices* (*VDI*) and *index-driven with pairs* (*IDP*).

4.1. Algorithm

The method to approximate a given potential $\phi : \Omega_{\mathbf{X}} \to \mathbb{R}_0^+$ is explained by considering potentials represented as *VDI* because this structure is simpler, but the practical application follows the same idea as for any other alternative (such as *IDP*, for example). Let the *VBP* potential to approximate be denoted as V. Let us assume that it stores n different values, denoted as $v_1 \dots v_n$ in increasing order of size. As we mentioned in our description of *VBPs*, although each different value v_i is only stored once, the information about the set of corresponding indices (or configurations) is saved, where $\mathbf{S}_i$ is $n_i = |\mathbf{S}_i|$ (which means that n_i is the number of configurations in $\mathbf{S}_i$).

Definition 1. *The basic approximation step consists of reducing the number of values by applying a reduction operation. This operation replaces two consecutive values, v_i and v_{i+1}, with their weighted average. Reduction can generally be described using the following notation:*

- *v_a and v_b will be the values to reduce with $\mathbf{S}_a$ and $\mathbf{S}_b$ as their sets of indices, with $n_a = |\mathbf{S}_a|$ and $n_b = |\mathbf{S}_b|$.*
- *v_r is the new value that replaces v_a and v_b, with $\mathbf{S}_r = \mathbf{S}_a \cup \mathbf{S}_b$ and $n_r = |\mathbf{S}_r|$. This value is computed as:*
$$v_r = \frac{n_a \cdot v_a + n_b \cdot v_b}{n_a + n_b}.$$
- *It is important to observe that this operation does not modify the total sum of the potential values. Therefore, if ϕ is the original potential and V the result of successive reductions, then $sum(\phi) = sum(V)$.*

Consequently, at the end of this operation, the number of values is reduced. The complete algorithm employed for approximating V_ϕ can now be intuitively described as follows:

1 There are a number of different approximation alternatives resulting in candidate structures which will become the one chosen for the final approximation. As there are n different values, there will be $n-1$ candidate structures produced by reducing every pair of consecutive values. Iterate from $i = 1$ to $i = n-1$:
   1.1 Let us consider two successive values: v_i and v_{i+1}. The candidate structure is then obtained by reducing both values as previously explained in Definition 1. The result of this operation will be V_i.
   1.2 Calculate the Kullback–Leibler divergence between the original potential V and V_i. This value is denoted by $D(V, V_i)$.

2 Select the candidate structure $V_m = \arg\min_{j=1\ldots n-1} D(V, V_j)$.

3 Repeat the previous steps until the selected stopping condition has been satisfied.

Before presenting a detailed description of the algorithm, we wish to include a number of considerations:

- It is evident that it is not necessary to build the candidate structures but only to evaluate the loss of information of the corresponding *reduction* operations.
- The Kullback–Leibler divergence between a candidate structure V_i and the original one can be computed by taking into account only those values and indices involved in the *reduction*, and the measure to compute is in fact the loss of information produced by this operation. The way to compute this measure will be explained below.
- A possible stopping criteria (this is the one used in the experimental work although others could be considered) consists of setting a global information loss threshold, t_l. Therefore, the procedure of reducing consecutive values will continue as long as the addition of information losses does not reach the threshold t_l.

4.2. Theoretical Background

Let us consider a potential $\phi(\mathbf{X})$ where $V(\mathbf{X})$ is its representation as *VBP*. The degree of approximation between them will be measured with the Kullback–Leibler divergence [21] between the corresponding normalized potentials ($\overline{\phi}$ and $\overline{V}$):

$$D(\phi, V) = \sum_{\mathbf{x} \in \Omega_\mathbf{X}} \overline{\phi}(\mathbf{x}) log \frac{\overline{\phi}(\mathbf{x})}{\overline{V}(\mathbf{x})}. \tag{6}$$

The divergence is a non-negative real number which would only be equal to zero if V provides an exact representation of ϕ. As we explained previously, the key operation for approximating ϕ represented as V is *reduction*, as described in Definition 1 and Algorithm 1.

Algorithm 1 Approximation of a potential ϕ represented as V (*VBP*).

function APPROXIMATE(V, t_l) ▷ t_l: global loss threshold
  $loss \leftarrow 0$
  while $loss < t_l$ **do** ▷ loss threshold is not reached
    $n \leftarrow$ number of values in ϕ
    for $i \in \{1, ..., n-1\}$ **do**
      consider the reduction of v_i and v_{i+1}
      // compute information loss in V due to reduction
      compute $I(V, \mathbf{S}_i, \mathbf{S}_{i+1})$
    end for
    choose V_m which minimizes $I(V, \mathbf{S}_i, \mathbf{S}_{i+1}), i = 1 \dots n-1)$
    $loss \leftarrow loss + I(V, \mathbf{S}_m, \mathbf{S}_{m+1})$
    $V \leftarrow V_m$ ▷ keeps reducing V if possible
  end while
  return V ▷ return V after reaching the loss threshold
end function

Definition 2. *Let us use V_j to denote the approximated VBP structure obtained in the j-th iteration of the algorithm under consideration in the $j+1$-th iteration. The new reduction to consider will be described in the previously presented terms. The* ***information loss*** *produced by this* ***reduction*** *is defined as:*

$$I(V_j, \mathbf{S}_a, \mathbf{S}_b) = D(\phi, V_j) - D(\phi, V_{j+1}). \tag{7}$$

The selection of the pair of values minimizing the information loss will consequently lead to the minimum value of the Kullback–Leibler divergence between the original potential and the approximate one.

Proposition 1. *The information loss obtained by reducing v_a and v_b in V can be computed as follows:*

$$I(V, \mathbf{S}_a, \mathbf{S}_b) = \frac{1}{sum(V)} \left[log(v_r) sum(V^{\downarrow \mathbf{S}_r}) - log(v_a) sum(V^{\downarrow \mathbf{S}_a}) - log(v_b) sum(V^{\downarrow \mathbf{S}_b}) \right]. \tag{8}$$

where $sum(V)$ denotes the addition of every value of V and $V^{\downarrow \mathbf{S}}$ represents the potential V restricted to the configurations included in $\mathbf{S}$ and all remaining values are discarded. If we consider ϕ to be the original potential and V its representation as VBP (perhaps after applying several reduction operations), then $sum(\phi) = sum(V)$ and the previous equation can be expressed as:

$$I(V, \mathbf{S}_a, \mathbf{S}_b) = \frac{1}{sum(\phi)} \left[log(v_r) sum(\phi^{\downarrow \mathbf{S}_r}) - log(v_a) sum(\phi^{\downarrow \mathbf{S}_a}) - log(v_b) sum(\phi^{\downarrow \mathbf{S}_b}) \right]. \tag{9}$$

Proof. Let ϕ be a potential represented by V (a *VBP*). V_j denotes the potential obtained from V as a result of the j-th iteration of the approximation algorithm. According to Definition 2:

$$I(V_j, \mathbf{S}_a, \mathbf{S}_b) = D(\phi, V_j) - D(\phi, V_{j+1}). \tag{10}$$

This difference can be calculated by separating the configurations defined in $\mathbf{X}$ into three different subsets: $\Omega_{\mathbf{X}} = \{\Omega_{\mathbf{X}} \setminus \mathbf{S}_r\} \cup \mathbf{S}_a \cup \mathbf{S}_b$:

$$
\begin{aligned}
I(V_j, \mathbf{S}_a, \mathbf{S}_b) = D(\phi, V_j) - D(\phi, V_{j+1}) = \\
\sum_{\mathbf{x} \in \{\Omega_{\mathcal{X}} \setminus \mathbf{S}_r\}} \left[\overline{\phi}(\mathbf{x}) log(\frac{\overline{\phi}(\mathbf{x})}{\overline{V}_j(\mathbf{x})}) - \overline{\phi}(\mathbf{x}) log(\frac{\overline{\phi}(\mathbf{x})}{\overline{V}_{j+1}(\mathbf{x})}) \right] + \\
\sum_{\mathbf{x} \in \mathbf{S}_a} \left[\overline{\phi}(\mathbf{x}) log(\frac{\overline{\phi}(\mathbf{x})}{v_a / sum(\phi))} - \overline{\phi}(\mathbf{x}) log(\frac{\overline{\phi}(\mathbf{x})}{v_r / sum(\phi)}) \right] + \\
\sum_{\mathbf{x} \in \mathbf{S}_b} \left[\overline{\phi}(\mathbf{x}) log(\frac{\overline{\phi}(\mathbf{x})}{v_b / sum(\phi))} - \overline{\phi}(\mathbf{x}) log(\frac{\overline{\phi}(\mathbf{x})}{v_r / sum(\phi)}) \right].
\end{aligned} \tag{11}
$$

It should be noted that the first part of the summation is equal to 0 since the values of the configurations that are not involved in the reduction ($\mathbf{x} \in \Omega_{\mathbf{X} \setminus \mathbf{S}_r}$) are identical in V_j and V_{j+1}. Additionally, when the properties of the logarithm are considered, the previous equation can be expressed as follows:

$$
\begin{aligned}
\sum_{\mathbf{x} \in \mathbf{S}_a} \overline{\phi}(\mathbf{x}) \left[log(\overline{\phi}(\mathbf{x})) - log(\frac{v_a}{sum(\phi)}) - log(\overline{\phi}(\mathbf{x})) + log(\frac{v_r}{sum(\phi)}) \right] + \\
\sum_{\mathbf{x} \in \mathbf{S}_b} \overline{\phi}(\mathbf{x}) \left[log(\overline{\phi}(\mathbf{x}) - log(\frac{v_b}{sum(\phi)}) - log(\overline{\phi}(\mathbf{x})) + log(\frac{v_r}{sum(\phi)}) \right] = \\
\sum_{\mathbf{x} \in \mathbf{S}_a} \overline{\phi}(\mathbf{x}) log(\frac{v_r}{v_a}) + \sum_{\mathbf{x} \in \mathbf{S}_b} \overline{\phi}(\mathbf{x}) log(\frac{v_r}{v_b}).
\end{aligned} \tag{12}
$$

Since $\overline{\phi}(\mathbf{x}) = \dfrac{\phi(\mathbf{x})}{sum(\phi)}$ and if we remove the logarithm from the sum as it does not depend on the configurations, the previous equation can then be written as follows:

$$
\begin{aligned}
log(\frac{v_r}{v_a}) \sum_{\mathbf{x} \in \mathbf{S}_a} \frac{\phi(\mathbf{x})}{sum(\phi)} + log(\frac{v_r}{v_b}) \sum_{\mathbf{x} \in \mathbf{S}_b} \frac{\phi(\mathbf{x})}{sum(\phi)} = \\
\frac{1}{sum(\phi)} \left[log(v_r) sum(\phi^{\downarrow \mathbf{S}_a}) - log(v_a) sum(\phi^{\downarrow \mathbf{S}_a}) + log(v_r) sum(\phi^{\downarrow \mathbf{S}_b}) - log(v_b) sum(\phi^{\downarrow \mathbf{S}_b}) \right] = \\
\frac{1}{sum(\phi)} \left[log(v_r) sum(\phi^{\downarrow \mathbf{S}_r}) - log(v_a) sum(\phi^{\downarrow \mathbf{S}_a}) - log(v_b) sum(\phi^{\downarrow \mathbf{S}_b}) \right].
\end{aligned} \tag{13}
$$

□

4.3. Example

The application of the approximation algorithm will be exemplified using the potential presented in Example 1 and stored as a *VDI*, as shown in Figure 10. The practical implementation of the algorithm attempts to simplify computations as much as possible. Therefore, the global sum of the potential values in Equation (8) can be avoided, as it is not needed for determining the candidate structure with lower loss of information.

As the potential stores 6 different probability values, the initial iteration must therefore consider 5 candidate structures, i.e., 5 different *reduction* operations, and then calculate their respective information losses. This information is presented in Table 1. Each row considers the values to be reduced (v_a and v_r) and the new value (v_r) in addition to their corresponding sets of indices ($\mathbf{S}_a$, $\mathbf{S}_b$ and $\mathbf{S}_r$). The alternative with the lowest information loss is presented in bold.

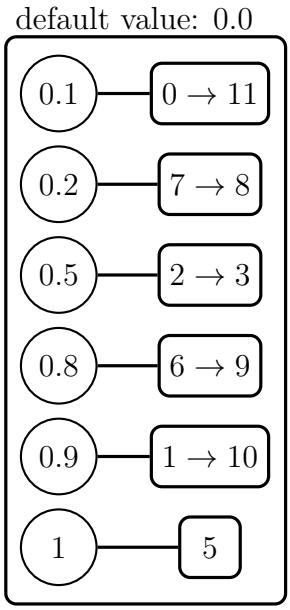

Figure 10. Potential to approximate.

Table 1. Candidate structures for the first iteration. Bold typeface is used for the preferred candidate structure.

$v_a - \mathbf{S}_a$	$v_b - \mathbf{S}_b$	$v_r - \mathbf{S}_r$	$I(V, \mathbf{S}_a, \mathbf{S}_b)$
$0.1 - \{0, 11\}$	$0.2 - \{7, 8\}$	$0.15 - \{0, 7, 8, 11\}$	0.014757
$0.2 - \{7, 8\}$	$0.5 - \{2, 3\}$	$0.35 - \{2, 3, 7, 8\}$	0.057686
$0.5 - \{2, 3\}$	$0.8 - \{6, 9\}$	$0.65 - \{2, 3, 6, 9\}$	0.030339
$0.8 - \{6, 9\}$	$0.9 - \{1, 10\}$	$0.85 - \{1, 6, 9, 10\}$	0.002556
$\mathbf{0.9 - \{1, 10\}}$	$\mathbf{1 - \{5\}}$	$\mathbf{0.93333 - \{1, 5, 10\}}$	**0.001533**

Therefore, the preferred candidate structure is the final one and the resulting approximate structure is the one presented in Figure 11. The total loss is 0.001533.

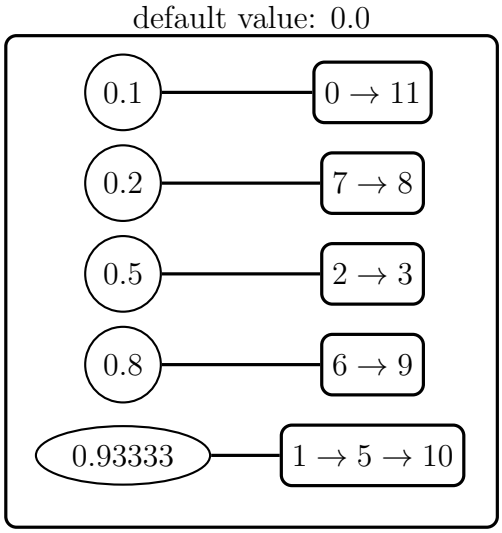

Figure 11. Approximation of ϕ obtained in the first iteration.

In the second iteration, there are only 4 candidate structures to consider, as shown in Table 2.

Table 2. Candidate structures for the second iteration. The best reduction is presented with bold typeface.

$v_a - \mathbf{S}_a$	$v_b - \mathbf{S}_b$	$v_r - \mathbf{S}_r$	$I(V, \mathbf{S}_a, \mathbf{S}_b)$
$0.1 - \{0, 11\}$	$0.2 - \{7, 8\}$	$0.15 - \{0, 7, 8, 11\}$	0.014757
$0.2 - \{7, 8\}$	$0.5 - \{2, 3\}$	$0.35 - \{2, 3, 7, 8\}$	0.057686
$0.5 - \{2, 3\}$	$0.8 - \{6, 9\}$	$0.65 - \{2, 3, 6, 9\}$	0.030339
$\mathbf{0.8 - \{6, 9\}}$	$\mathbf{0.93333 - \{1, 5, 10\}}$	$\mathbf{0.88 - \{1, 5, 6, 9, 10\}}$	**0.005323**

The *reduction* of the values 0.8 and 0.93333 therefore performs the best. The approximate structure after this iteration is presented in Figure 12. The global loss is now 0.006856.

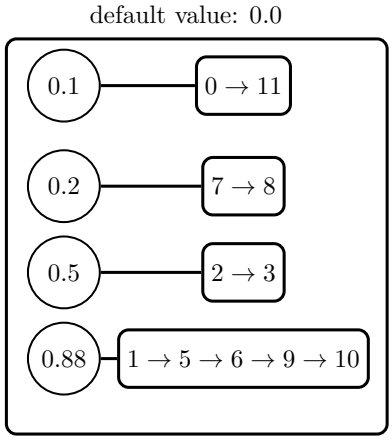

Figure 12. Approximation of ϕ obtained in the second iteration.

In the next step, we will consider a third iteration by selecting from among the candidate *reductions* presented in Table 3.

Table 3. Candidate structures for the third iteration. The best reduction is presented with bold typeface.

$v_a - \mathbf{S}_a$	$v_b - \mathbf{S}_b$	$v_r - \mathbf{S}_r$	$I(V, \mathbf{S}_a, \mathbf{S}_b)$
$\mathbf{0.1 - \{0, 11\}}$	$\mathbf{0.2 - \{7, 8\}}$	$\mathbf{0.15 - \{0, 7, 8, 11\}}$	**0.014757**
$0.2 - \{7, 8\}$	$0.5 - \{2, 3\}$	$0.35 - \{2, 3, 7, 8\}$	0.057686
$0.5 - \{2, 3\}$	$0.88 - \{1, 5, 6, 9, 10\}$	$0.65 - \{2, 3, 6, 9\}$	0.063298

If we combine the values 0.1 and 0.2, we obtain the new approximated potential shown in Figure 13.

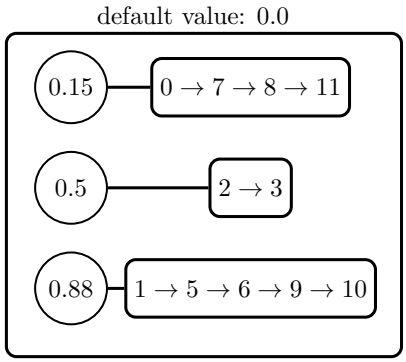

Figure 13. Final approximation of ϕ obtained in the third iteration.

The loss of information in relation to the original potential is now 0.021613. The next iteration must select between only two *reductions*, as shown in Table 4.

Table 4. Candidate structures for the fourth iteration.

$v_a - \mathbf{S}_a$	$v_b - \mathbf{S}_b$	$v_r - \mathbf{S}_r$	$I(V, \mathbf{S}_a, \mathbf{S}_b)$
$0.15 - \{0, 7, 8, 11\}$	$0.5 - \{2, 3\}$	$0.5333 - \{0, 2, 3, 7, 8, 11\}$	0.123074
$0.5 - \{2, 3\}$	$0.88 - \{1, 5, 6, 9, 10\}$	$0.65 - \{2, 3, 6, 9\}$	0.063298

If the global loss threshold is 0.05, then there are no more *reductions* to apply and the process ends with the approximate potential shown in Figure 13. We need to make one last comment about the operation of the algorithm. If we look at the tables, it is apparent that information loss values for each *reduction* remain constant, regardless of the other values. This facilitates the consideration of alternative structures by storing the already calculated loss values, thereby avoiding repeated computations.

5. Empirical Evaluation

The application of the approximation algorithm will be evaluated by considering various *BNs* developed for modeling medical problems. All of these are included in the *bnlearn* repository (see [17,18]) and are either categorized as large (*HEPAR II*) or very large (*diabetes*, *munin*, and *pathfinder*) networks. The main features of these are described below.

- The *hepar2* network was defined by A. Onisko in her Ph.D. dissertation [22] as part of the *HEPAR II* project. The project was inspired by the *HEPAR* system [23], the aim of which is to support the diagnosis of liver and biliary tract disorders.
- *pathfinder* ([24]) is a system which, when combined with expert knowledge from surgical pathologists, can assist in the diagnosis of lymphnode diseases. As a result of this study, the discrete *pathfinder* network was defined.
- The *munin* network was defined while creating the expert system identified by the same acronym *MUNIN* (MUscle and Nerve Inference Network) [25]. The aim of this system was to help electromyographics (EMCs), which are designed to localize and characterize lesions of the neuro-muscular system, from a patho-physiological approach combined with expert knowledge.
- The *diabetes* [26] *BN* represents a differential equation model which attempts to adjust the insulin therapy for diabetic people. The model considers the patient's state by measuring blood glucose, biologically active insulin, and the amount of undigested carbohydrate within an hour gap in addition to other known variables involved in the glucose metabolism process. The *diabetes* network enabled predictions to be extended to 24-hour blood glucose profiles and the insulin treatment to be adjusted.

Table 5 presents a summary of the information for each network: number of nodes, number of arcs, number of parameters (np), average *Markov blanket (M.B.)* size, *average degree*, and *maximum in-degree*. The networks are ordered according to the number of parameters because this is the most relevant feature in terms of the experimental work.

Table 5. *Bayesian network* features.

Network	Nodes	arcs	np	avg. M.B. Size	avg. deg	Max. in-deg
hepar2	70	123	2139	4.51	3.51	6
pathfinder	223	338	97,851	5.61	3.03	6
munin	1041	1397	98,423	3.54	2.68	3
diabetes	413	606	461,069	3.97	2.92	2

The experimental section is organized in the following way:

1. Analysis of the memory space necessary to store the complete networks using the different representation alternatives in order to compare it with the representation using 1DA, since this is considered to be the base representation (see Section 5.1).

2. Analysis of the main characteristics of the specific potentials of some variables that will later be used to perform inference, as well as the memory space necessary for their representation with the different structures considered (see Section 5.2).
3. Examination of the effect of the approximation on the memory space necessary for the storage of each network (see Section 5.3). The relationship with the memory space required by the base representation is determined, as well as the reduction produced in relation to the alternative representations but without any approximation. In this case, the results are presented by means of a specific table for each network in order to collect the information on the threshold values considered.
4. Propagation errors produced by the approximation, both local (only the potential of the target variable is approximated) and global (all potentials are approximated) (see Section 5.4). A table is presented for each network and this collects the results for the selected variables and for the set of thresholds used.
5. In order to obtain further information about the effect of the approximation, some charts are also included to show the effect of the approximation on the order of the probabilities of the marginal distributions obtained as a result of the propagation. If these distributions are used to make decisions, it is important that the alternatives are kept in the same order (according to their probability value) in which they appear in the exact result, without approximation (see Section 5.5).

5.1. Global Memory Size Analysis

This section analyzes the networks in order to determine the necessary memory size for each form of representation being considered: *1DA*, *PT*, *PPT*, *VDI*, and *IPD*. This part serves to check the convenience of using alternative *VBP*-type representations in networks modeling real-world medical problems. In this way, a base memory size is available and it will enable the effect of the approximation on memory spaces required for the *VBP*-type representations to be subsequently checked. Table 6 includes the following information:

- *network*: name of the network;
- *1DA*: memory size indispensable for *1DA* storing the complete set of potentials;
- *PT*: memory size required for *PT* representation and the saving or increase in space in terms of *1DA*. This last value is included in the second line and is computed as

$$\frac{as * 100}{bs} - 100, \tag{14}$$

  where *as* refers to the memory size of the alternative representation, and *bs* to the memory size of the *1DA* representation;
- *PPT*, *VDI*, and *IDP*: the same as the previous line for the remaining representations: pruned probability trees, *VDI* and *IDP*.

In Table 6, the best savings values are shown in bold. The results show that *VBP* structures behave better than *PT* and *PPT* in every network, although in some of these there are no savings in terms of the space required for the simplest representation of all: *1DA*. Some more specific comments are included below:

- In *hepar2*, we can see that *PPT* offers little improvement in relation to *PT*, which indicates that in reality there are few repeated values that can be used by the *PPT* pruning operation. The *VDI* structure provides a saving of approximately 44% compared to *PT*, while *IPD* represents a saving of 62%.
- In the case of *pathfinder*, there are notable savings in relation to *1DA* and very important ones with respect to *PT* and *PPT*. The biggest savings come from the *VDI* structure.
- With respect to the *munin* network, *VDI* representation needs almost the same memory space as *1DA* and there is a saving of about 23% in *IDP* (moreover, significant reductions can also be seen with respect to *PT* and *PPT*).
- Finally, for *diabetes*, both *VBP* structures represent a substantial reduction in memory space and this is slightly greater in the case of *VDI*.

Table 6. Global memory size analysis. Bold typeface denotes the structure with the best saving percentage (or with the smallest increase percentage).

Network	1DA	PT	PPT	VDI	IDP
hepar2	32,530	132,026 305.8592	131,756 305.0292	74,070 127.6975	49,602 **52.4808**
pathfinder	806,982	4,249,768 426.6249	3,779,470 368.3463	301,602 **−62.6259**	482,438 −40.2170
munin	994,672	3,393,878 241.2057	3,353,900 237.1865	997,864 0.3209	766,072 **−22.9825**
diabetes	3,773,200	10,044,948 166.2183	10,044,810 166.2146	964,380 **−74.4413**	1,105,728 −70.6952

In short, these data show the capacity of these structures to offer efficient mechanisms for representing quantitative information, and, as will be seen below, they allow the use of the approximation operation with the possibility of achieving additional memory savings.

5.2. Local Memory Size Analysis

This experiment gathers information about the selected variables of each network in order to determine their features and verify the relationship between representation and memory size. These variables will later be used as target variables using the *VE* algorithm ([27–29]) to compute their marginal distributions. The columns included in Table 7 are:

- *network*: name of the network;
- *variable*: name of the variable being examined;
- *np*: global number of parameters of the target variable potential;
- *nd*: number of different values in the potential (these are the values actually stored in the *VBP* representation);
- *1DA*: memory size for the *1DA* representation;
- *PT*: memory size required for *PT* representation and saving or increase regarding *1DA*. This last value is included in the second line and computed as before;
- *PPT*, *VDI*, and *IDP*: the same as the previous line for *PPT*, *VDI*, and *IDP*.

In this experiment, we have selected the variables with the largest number of parameters: *hepar2* (*ggtp*, *ast*, *alt*, and *bilirubin*); *pathfinder* (*F39*, *F74*, and *F40*); *munin* (*v1* (*L_LNLPC5_DELT_MUSIZE*), *v2* (*L_LNLE_ADM_MUSIZE*), and *v3* (*L_MED_ALLCV_EW*)); and *diabetes* (*cho_0*, *cho_1*, and *cho_2*). The best savings values are shown in bold. We wish to make the following comments about the results in Table 7:

- In *hepar2* variables, the number of different probability values is slightly lower than the number of parameters. This justifies the fact that memory space requirements do not reduce those required by *1DA*, although they do offer significant savings with respect to *PT* and *PPT*.
- Selected *pathfinder* variables present a high degree of repetition, so the number of different values is significantly lower than the number of parameters. This produces very significant memory savings in relation to *1DA* which are larger in the case of *VDI*.
- For the first two *munin* variables, there are only 12 different values but 600 parameters. This accounts for the notable memory space savings for *VBP* structures. In the case of the third variable, there are more different values (133), although this does suppose a high degree of repetition compared to the 600 necessary parameters.
- *Diabetes* variables have similar characteristics: only 45 different values (and 7056 possible values). Consequently, the memory space savings are very noticeable and appreciably better in the case of *VDI*.

Table 7. Local memory size analysis. Numbers in bold typeface denotes the best saving percentages (or with the smallest increase percentage).

Network	Variable	np	nd	1DA	PT	PPT	VDI	IDP
hepar2	ggtp	384	334	3454	19,452 463.1731	19,452 463.1731	9990 189.2299	6150 **78.0544**
	ast	288	231	2636	13,648 417.7542	13,648 417.7542	7084 168.7405	4508 **71.0167**
	alt	288	249	2636	13,648 417.7542	13,648 417.7542	7516 185.1290	4652 **76.4795**
	bilirubin	288	244	2636	13,426 409.3323	13,426 409.3323	7396 180.5766	4612 **74.9621**
pathfinder	F39	8064	30	64,794	376,442 480.9828	359,850 455.3755	15,114 **−76.6738**	28,698 −55.7089
	F74	7560	111	60,712	293,736 383.8187	152,072 150.4810	28,676 **−52.7672**	52,632 −13.3087
	F40	4032	43	32,488	116,076 257.2888	114,588 252.7087	5640 **−82.6397**	9280 −71.4356
munin	v1	600	12	5032	19,132 280.2067	19,132 280.2067	1112 **−77.9014**	1464 −70.9062
	v2	600	12	5032	19,132 280.2067	19,132 280.2067	1112 **−77.9014**	1464 −70.9062
	v3	600	133	4982	15,012 201.3248	15,012 201.3248	4066 −18.3862	2582 **−48.1734**
diabetes	cho_0	7056	45	56,630	139,546 146.4171	139,546 146.4171	9454 **−83.3057**	16,878 −70.1960
	cho_1	7056	45	56,630	139,546 146.4171	139,546 146.4171	9454 **−83.3057**	16,878 −70.1960
	cho_2	7056	45	56,630	139,546 146.4171	139,546 146.4171	9454 **−83.3057**	16,878 −70.1960

5.3. Global Memory Size with Approximation

This experiment considers the effect of the approximation on every potential in the network in terms of the necessary memory space after approximating with different thresholds. This determines the degree to which the approximation enables a reduction in the memory size for storing the networks. The results for this section are divided into various tables, one for each network (Tables 8–11), and all have a similar structure.

- The first column shows the threshold.
- The second presents data relating to the *VDI* structure: memory size after approximation, savings over *1DA* and savings with respect to the exact *VDI* representation.
- The third column is identical to the second but with data for the *IDP* structure.

5.3.1. *hepar2* Network

The number of parameters is 2139, and the memory sizes of *1DA*, *PT*, and *PPT* structures are 32,530, 132,026, and 131,756, respectively. Table 8 includes savings when approximation is applied.

Table 8. *hepar2*—Global approximation memory size analysis.

Threshold	VDI	IDP
0.00001	63,846 (96.2681/−13.8032)	46,194 (42.0043/−6.8707)
0.00005	58,062 (78.4875/−21.6120)	44,266 (36.0775/−10.7576)
0.00010	55,302 (70.0031/−25.3382)	43,346 (33.2493/−12.6124)
0.00050	48,558 (49.2714/−34.4431)	41,098 (26.3388/−17.1445)
0.00100	45,678 (40.4181/−38.3313)	40,138 (23.3876/−19.0799)
0.00500	39,798 (22.3425/−46.2697)	38,178 (17.3624/−23.0313)
0.01000	37,518 (15.3335/−49.3479)	37,418 (15.0261/−24.5635)
0.05000	33,798 (3.8979/−54.3702)	36,178 (11.2143/−27.0634)
0.10000	32,550 (0.0615/−56.0551)	35,762 (9.9354/−27.9021)

Table 9. *pathfinder*—Global approximation memory size analysis.

Threshold	VDI	IDP
0.00001	293,178 (−63.6698/−2.7931)	479,630 (−40.5650/−0.5820)
0.00005	290,682 (−63.9791/−3.6207)	478,798 (−40.6681/−0.7545)
0.00010	289,266 (−64.1546/−4.0902)	478,326 (−40.7266/−0.8523)
0.00050	285,450 (−64.6275/−5.3554)	477,054 (−40.8842/−1.1160)
0.00100	283,170 (−64.9100/−6.1114)	476,294 (−40.9784/−1.2735)
0.00500	277,002 (−65.6743/−8.1564)	474,238 (−41.2331/−1.6997)
0.01000	274,050 (−66.0401/−9.1352)	473,254 (−41.3551/−1.9037)
0.05000	267,090 (−66.9026/−11.4429)	470,934 (−41.6426/−2.3846)
0.10000	264,450 (−67.2298/−12.3182)	470,054 (−41.7516/−2.5670)

Table 10. *munin*—Global approximation memory size analysis.

Threshold	VDI	IDP
0.00001	880,744 (−11.4538/−11.7371)	727,032 (−26.9074/−5.0961)
0.00005	829,096 (−16.6463/−16.9129)	709,816 (−28.6382/−7.3434)
0.00010	800,584 (−19.5128/−19.7702)	700,312 (−29.5937/−8.5840)
0.00050	725,440 (−27.0674/−27.3007)	675,264 (−32.1119/−11.8537)
0.00100	692,296 (−30.3996/−30.6222)	664,216 (−33.2226/−13.2959)
0.00500	615,976 (−38.0725/−38.2705)	638,776 (−35.7802/−16.6167)
0.01000	587,848 (−40.9003/−41.0894)	629,400 (−36.7229/−17.8406)
0.05000	533,728 (−46.3413/−46.5130)	611,360 (−38.5365/−20.1955)
0.10000	518,272 (−47.8952/−48.0619)	606,208 (−39.0545/−20.8680)

Here are some comments about Table 8:

- For *VDI*, it is apparent that there is a very noticeable increase in memory space savings as the threshold used for the approximation becomes greater, reaching very similar sizes to those of *1DA* for the threshold 0.1. For every threshold, there is a reduction in relation to the exact *VDI* structure (without the use of approximation).
- With the *IDP* structure, the behavior is similar, although the reductions are not as notable as with *VDI*.

Table 11. *diabetes*—Global approximation memory size analysis.

Threshold	VDI	IDP
0.00001	843,180 (−77.6535/−12.5677)	1,065,328 (−71.7659/−3.6537)
0.00005	799,932 (−78.7996/−17.0522)	1,050,912 (−72.1480/−4.9575)
0.00010	776,868 (−79.4109/−19.4438)	1,043,224 (−72.3517/−5.6527)
0.00050	719,148 (−80.9406/−25.4290)	1,023,984 (−72.8617/−7.3928)
0.00100	694,908 (−81.5831/−27.9425)	1,015,904 (−73.0758/−8.1235)
0.00500	644,076 (−82.9302/−33.2135)	998,960 (−73.5249/−9.6559)
0.01000	626,172 (−83.4047/−35.0700)	992,992 (−73.6830/−10.1956)
0.05000	594,324 (−84.2488/−38.3724)	982,376 (−73.9644/−11.1557)
0.10000	585,636 (−84.4791/−39.2733)	979,480 (−74.0411/−11.4176)

5.3.2. *pathfinder* Network

This contains 97,851 parameters, and the memory sizes for *1DA*, *PT*, and *PPT* are 806,982, 4,249,768, and 3,779,470. The memory sizes for several degrees of approximation are presented in Table 9.

It is worth remembering that in this network, the *VDI* structure without approximation already represented a saving of approximately 62.7% in relation to *1DA*, which increases as the threshold value grows. For the highest threshold value, the saving is 12.3% with respect to the *VDI* structure without approximation. Similar results can be observed for *IDP*.

5.3.3. *munin* Network

This network requires 994,672 parameters to store the quantitative information and the memory sizes required for alternative representation structures with approximation operation are 994,672, 3,393,878, and 3,353,900 for *1DA*, *PT*, and *PPT*. The effect of approximation can be observed in Table 10.

In this network, the reduction of space is extremely notable both with respect to *1DA* and also to the exact representations through *VDI* and *IDP*, although the reduction is more important in the case of *VDI*.

5.3.4. *diabetes* Network

In the *diabetes* network, the number of parameters is 461,069, and the memory sizes for representations as *1DA*, *PT*, and *PPT* are 3,773,200, 10,044,948, and 10,044,810. The effect of approximation in memory sizes is presented in Table 11.

As in the case of the *munin* network, memory size reductions are important and especially relevant for *VDI*.

5.4. Propagation Errors with Approximation

The objective of this part is to check the effect of approximation on propagation errors using the *VE* algorithm on the set of selected variables. For each target variable, two different values are presented: the error when approximation is limited to the potential of the target variable and when approximation is applied to the entire set of potentials. As *VDI* and *IDP* approximations will produce the same potentials, this experiment will be performed exclusively on the *VDI* representation. The steps followed to produce the results are:

1. Perform a *VE* propagation on each target variable for storing the marginal obtained as the ground result V_g.
2. Modify the network by approximating the potential of the target variable, saving the remaining ones as defined in the network specification.
3. Perform a second *VE* propagation on the modified network setting the selected target variable. The result is termed as V_{la}.
4. Apply the approximation on the entire set of potentials.

5. Compute a third *VE* propagation for the selected variable, producing V_{ga}.
6. Compute the divergences between the ground result and the approximate ones: $D(V_g, V_{la})$ and $D(V_g, V_{ga})$.

In order to introduce the results obtained, Tables 12–15 are organized as follows. Threshold values are presented in the first column; for each variable the *local* columns contain the errors of propagation with approximation on target variable, that is $D(V_g, V_{la})$; and *global* columns show the errors of propagation when approximation is applied on all the potentials ($D(V_g, V_{ga})$). It should be noted that the values presented in the following tables are rounded to include only three decimal places. Therefore, the value of divergence $d_l = 0.001$ will be referred to as the limit value.

5.4.1. *hepar2* Network

It is apparent that if the threshold value is below 0.005, then the errors remain below d_l. Errors above this threshold value only appear for the last three threshold values, and even for these values there are variables in which both the global and local approximations remain below d_l. The largest error value is 0.005 (quite small) for the *ggtp* variable in the case of global approximation with a threshold value of 0.1.

Table 12. *hepar2*—local and global approximation propagation error analysis.

Threshold	ggtp		ast		alt		bilirubin	
	Local	Global	Local	Global	Local	Global	Local	Global
0.00001	0.000	0.000	0.000	0.000	0.000	0.000	0.000	0.000
0.00005	0.000	0.000	0.000	0.000	0.000	0.000	0.000	0.000
0.00010	0.000	0.000	0.000	0.000	0.000	0.000	0.000	0.000
0.00050	0.000	0.000	0.000	0.000	0.000	0.000	0.000	0.000
0.00100	0.000	0.000	0.000	0.000	0.000	0.000	0.000	0.000
0.00500	0.000	0.000	0.000	0.000	0.000	0.000	0.000	0.000
0.01000	0.000	0.001	0.000	0.000	0.000	0.000	0.000	0.001
0.05000	0.002	0.004	0.001	0.001	0.000	0.000	0.000	0.001
0.10000	0.002	0.005	0.003	0.004	0.001	0.002	0.001	0.001

Table 13. *pathfinder*—local and global approximation propagation error analysis.

Threshold	F39		F74		F40	
	Local	Global	Local	Global	Local	Global
0.00001	−0.000	0.000	0.000	0.000	0.000	0.000
0.00005	0.000	0.000	0.000	0.000	0.000	0.000
0.00010	0.000	0.000	0.000	0.000	0.000	0.000
0.00050	0.000	0.000	0.000	0.000	0.000	0.000
0.00100	0.000	0.000	0.000	0.000	0.000	0.000
0.00500	0.000	0.000	0.000	0.000	0.000	0.000
0.01000	0.000	0.000	0.000	0.000	0.000	0.000
0.05000	0.000	0.004	0.000	0.000	0.000	0.005
0.10000	0.000	0.005	0.000	0.001	0.000	0.006

Table 14. munin—local and global approximation propagation error analysis.

Threshold	v1		v2		v3	
	Local	Global	Local	Global	Local	Global
0.00001	0.000	0.000	0.000	0.000	0.000	0.000
0.00005	0.000	0.000	0.000	0.000	0.000	0.000
0.00010	0.000	0.000	0.000	0.000	0.000	0.000
0.00050	0.000	0.000	0.000	0.000	0.000	0.001
0.00100	0.000	0.000	0.000	0.000	0.000	0.001
0.00500	0.000	0.001	0.000	0.001	0.000	0.005
0.01000	0.000	0.001	0.000	0.001	0.000	0.006
0.05000	0.000	0.002	0.000	0.003	0.000	0.096
0.10000	0.000	0.002	0.000	0.003	0.000	0.093

Table 15. diabetes—local and global approximation propagation error analysis.

Threshold	cho_0		cho_1		cho_2	
	Local	Global	Local	Global	Local	Global
0.00001	0.000	0.000	0.000	0.000	0.000	0.000
0.00005	0.000	0.000	0.000	0.000	0.000	0.000
0.00010	0.000	0.000	0.000	0.000	0.000	0.000
0.00050	0.001	0.001	0.000	0.001	0.000	0.000
0.00100	0.001	0.001	0.000	0.001	0.000	0.000
0.00500	0.001	0.001	0.000	0.000	0.000	0.000
0.01000	0.001	0.001	0.000	0.000	0.000	0.000
0.05000	0.000	0.000	0.000	0.001	0.000	0.000
0.10000	0.001	0.001	0.001	0.002	0.000	0.002

5.4.2. *pathfinder* Network

The results for this network are similar to those obtained for the *hepar2* network. All errors are below d_l for threshold values between 0.00001 and 0.01. Even above these values, the local approximation produces errors that are below d_l in every variable. The largest error occurs for the threshold 0.1 and global approximation for the variable *F40*.

5.4.3. *munin* Network

In the case of the *munin* network, there are only significant errors for the case of global approximation and with high thresholds (0.0096 for threshold 0.05 and 0.093 for threshold 0.1 and variable *v3*). The local approximation always produces error values lower than the limit value d_l.

5.4.4. *diabetes* Network

For the *diabetes* network, the variable *cho_0* is the one that offers the worst results, with errors equal to the limit value d_l in the case of local approximation and with threshold values over 0.0005. In any case, all the error values are very small, even for global approximation and large threshold values.

5.5. Order of Preferences

As stated earlier, the results of propagation can be used to aid in a decision-making process. It is therefore important that the errors are kept low (as demonstrated by the previous experiments) but that the order between the probability values of the states of the

variables on which the propagation is performed is also maintained. In the charts included in this experimentation (see Tables 16–20), the possible states of the variables are denoted as si. Let us imagine a variable with the three states: $s1, s2, s3$. Let us also suppose that exact propagation indicates that the order of the states according to their probability, from highest to lowest, is $s2, s11, s3$. This will therefore be the order of preferences that should be maintained so that the decision does not change as a result of errors produced by the approximation. In this way, the ideal situation will be one in which the order of preferences is not altered despite the approximation made, whether global or local. The colors in the tables also represent the differences between the probability values obtained for each alternative (with respect to the probability values obtained in the exact propagation), with colors ranging from green for the lowest differences to red for the highest values and those in between in varying shades of yellow.

Table 16. Preferences for *hepar2* variables.

Table 17. Preferences for *pathfinder* variables.

F39	F74	F40
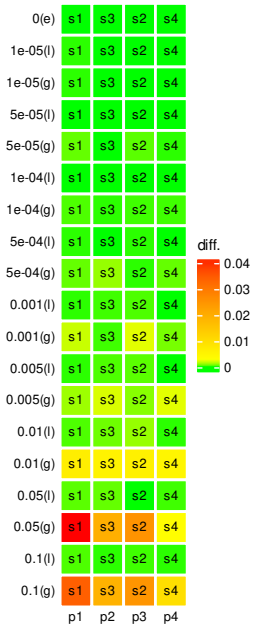	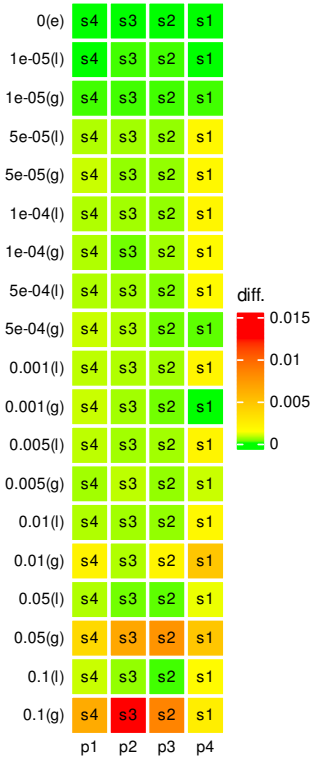	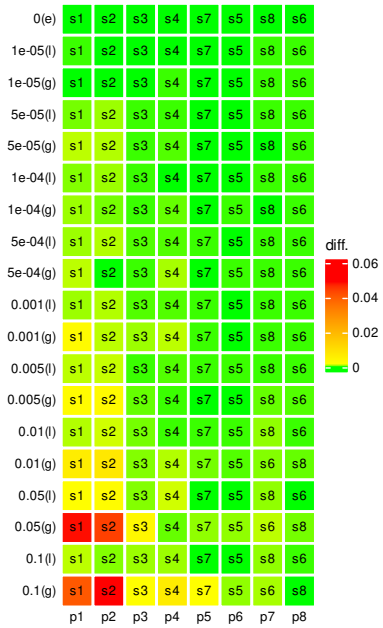

Table 18. Preferences for *munin* variables.

L_LNLPC5_DELT_MUSIZE	L_LNLE_ADM_MUSIZE	L_MED_ALLCV_EW
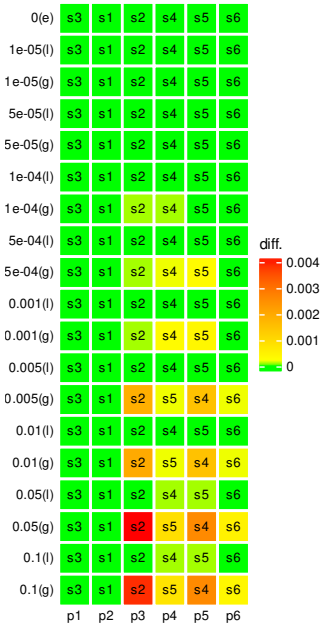	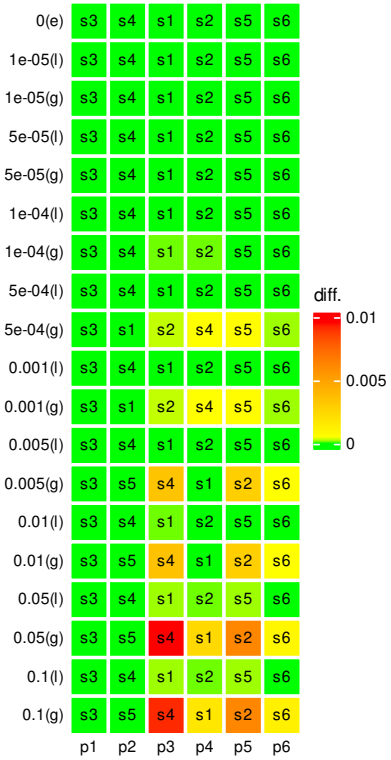	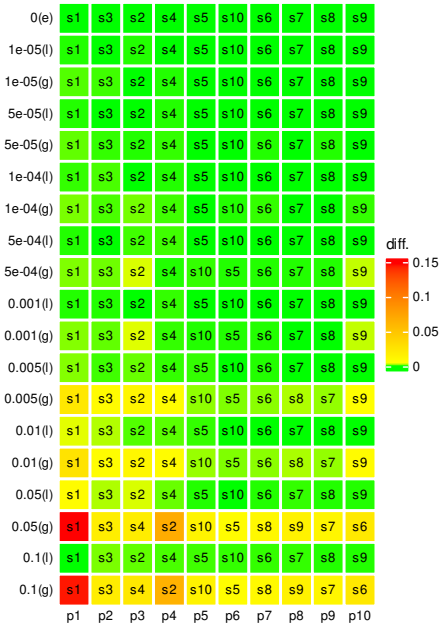

Table 19. Preferences for *cho_0* and *cho_1*.

cho_0

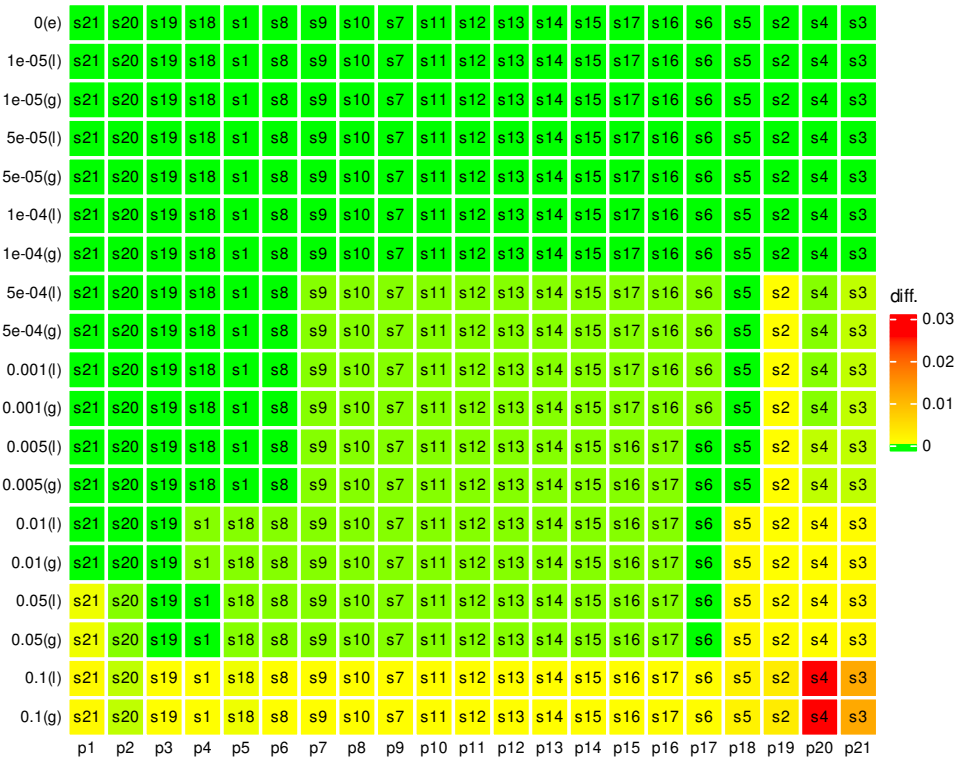

cho_1

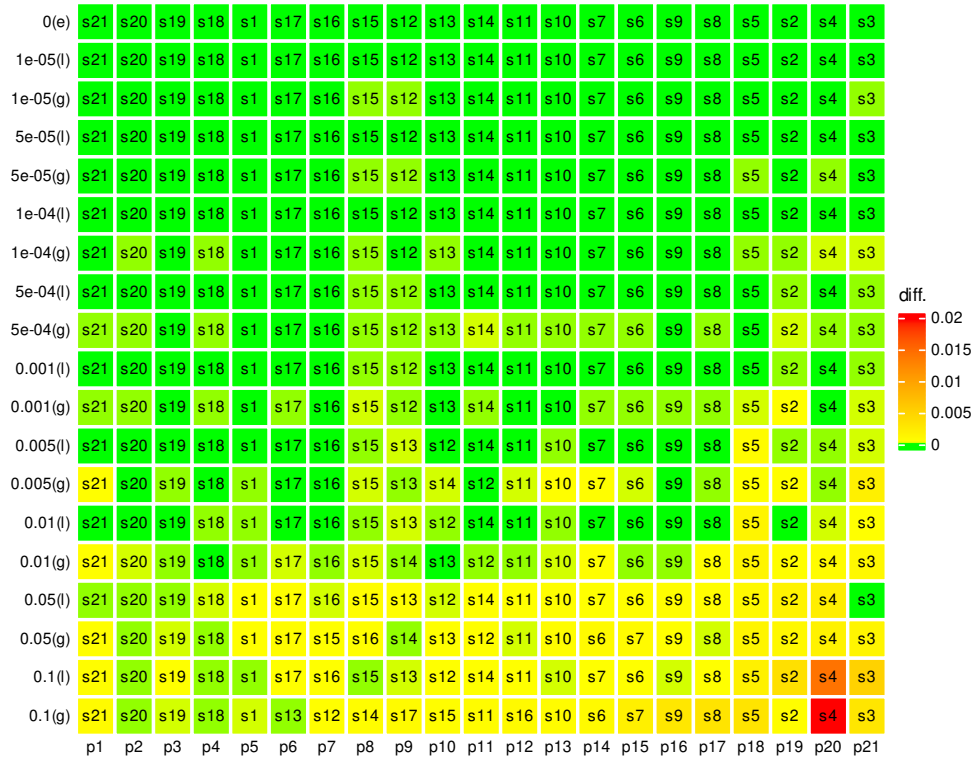

Table 20. Preferences for *cho_2*.

cho_2

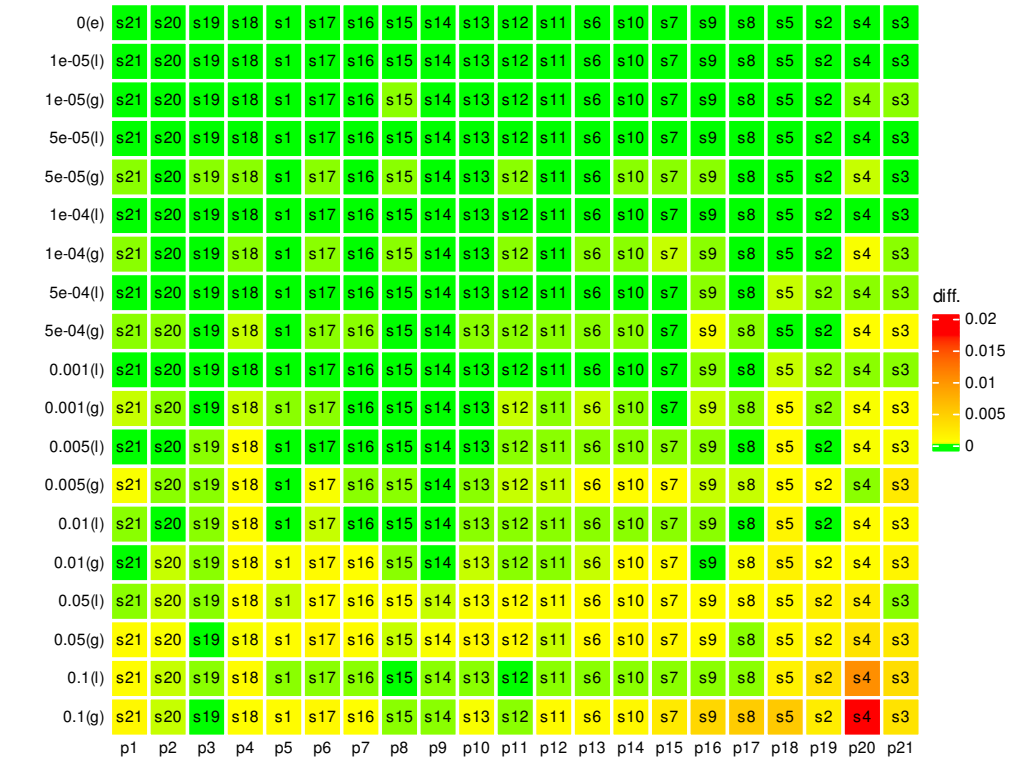

5.5.1. *hepar2* Network

For this network, the order of preferences ($s3, s3, s2, s1$ for *ggtp* and *bilirubin*, and $s3, s4, s2, s1$ for *ast* and *alt*) are always maintained, both for global and local approximation as well as for every threshold value. Similarly, it can be seen that the probability differences are always small, with maximum values of 0.04 for the case of the *ggtp* and *ast* variables.

5.5.2. *pathfinder* Network

For the three variables in this network, the same behavior is observed as in the case of the previous network: the preference orders are maintained for every threshold and for both forms of approximation. The largest probability difference value is 0.06 for the variable *F*40, and this appears in the global approximation case with the highest threshold values.

5.5.3. *munin* Network

For this network, there are changes in the order of preferences, although these do not affect the most probable alternatives. For the three variables, the changes appear with threshold values starting at 0.0005 and always for the case of global approximation. The highest values of probability difference occur for the third variable, reaching 0.15 with high thresholds and global approximation.

5.5.4. *diabetes* Network

The results for this network have been divided into two tables due to the number of states of the variables considered (21 in total).

For these two variables, there are changes in the orders of preferences for threshold values from 0.005 with both types of approximation. It should be noted that the differences between probability values are very low (the maximum is 0.02) and that the changes do not affect the first preferences (3 first in the case of *cho_0* and 6 first in the case of *cho_1*).

For the last variable, there are no changes in the preference orders and the difference between probability values is very small, even in the case of large thresholds and global approximation (the maximum value is 0.02).

6. Discussion

In this work, we have analyzed the characteristics of some *BNs* that model real medical problems. This analysis has allowed us to observe that the probability distributions that quantify the uncertainty of the problem have various common characteristics, and these include the fact that there are many impossible events and that some probability values tend to appear several times. For example, when analyzing the *pathfinder* network (see Table 7), it can be seen that although the probability distribution for the variable *F39* has 8064 parameters, there are only 30 different values for these. However, these repetitions do not always appear in a way that can be used by tree-like structures such as *PPT* or *BPT*. This justifies the use of the considered *VBP* structures, which in some cases enable a considerable saving of memory space in relation to other possible representation structures.

The need to deal with increasingly complex problems may subsequently lead to situations where models cannot be evaluated by exact inference algorithms, such as the *VE* algorithm. In such cases, our work considers the possibility of approximating the *VBP* structures, forcing an additional saving of space at the cost of losing information. Our work presents the way in which this operation should be carried out and experimentally demonstrates that the errors it induces in the results of the inference algorithms are small and that in many cases they do not alter the preference orders between variable alternatives. In this way, the decision-making process based on the approximate results would match the one performed if the exact propagation could be computed.

Author Contributions: Writing–review & editing, P.B.-N., A.C., M.G.-O., S.M. and O.P.R. All authors have read and agreed to the published version of the manuscript.

Funding: This paper is supported by the Spanish Ministry of Education and Science under project PID2019-106758GB-C31 and the European Regional Development Fund (FEDER). Funding for open access publication has been provided by the *Universidad de Granada/CBUA*.

Data Availability Statement: The software used in this paper was implemented in **Scala**. The code is available at https://github.com/mgomez-olmedo/VBPots (accessed on 15 June 2022).. This repository also stores the information required for reproducing the experiments.

Conflicts of Interest: The authors declare no conflict of interest.

Abbreviations

The following abbreviations are used in this manuscript:

BN	Bayesian network
BPT	Binary probability tree
DAG	Decision acyclic graph
ID	Influence diagram
IDM	Index-driven with map
IDP	Index-driven with pair of arrays
PGM	Probabilistic graphical model
PPT	Pruned probability tree
PT	Probability tree
VBP	Value-based potential
VDG	Value-driven with grains
VDI	Value-driven with indices
1DA	Unidimensional array

References

1. Koller, D.; Friedman, N. *Probabilistic Graphical Models: Principles and Techniques*; MIT Press: Cambridge, MA, USA, 2009.
2. Lauritzen, S.L. *Graphical Models*; Oxford University Press: Oxford, UK, 1996.
3. Pearl, J. *Probabilistic Reasoning in Intelligent Systems: Networks of Plausible Inference*; Morgan Kaufmann: Burlington, MA, USA, 1988.
4. Pearl, J. *Bayesian Networks: A Model of Self-Activated Memory for Evidential Reasoning*; Computer Science Department, University of California, California, LA, USA, 1985.
5. Pearl, J.; Russell, S. Bayesian Networks. Computer Science Department, University of California. 1998. Available online: https://people.eecs.berkeley.edu/~russell/papers/hbtnn-bn.pdf (accessed on 15 June 2022).
6. Howard, R.A.; Matheson, J.E. Influence diagram retrospective. *Decis. Anal.* **2005**, *2*, 144–147. [CrossRef]
7. Olmsted, S.M. On Representing and Solving Decision Problems. Ph.D. Thesis, Department of Engineering-Economic Systems, Stanford University, Stanford, CA, USA, 1983.
8. Arias, M.; Díez, F. Operating with potentials of discrete variables. *Int. J. Approx. Reason.* **2007**, *46*, 166–187. [CrossRef]
9. Boutilier, C.; Friedman, N.; Goldszmidt, M.; Koller, D. Context-specific independence in Bayesian networks. In Proceedings of the 12th Annual Conference on Uncertainty in Artificial Intelligence (UAI-96), Portland, OR, USA, 1–3 August 1996; pp. 115–123.
10. Cabañas, R.; Gómez, M.; Cano, A. Using binary trees for the evaluation of influence diagrams. *Int. J. Uncertain. Fuzziness Knowl. Based Syst.* **2016**, *24*, 59–89. [CrossRef]
11. Cano, A.; Moral, S.; Salmerón, A. Penniless propagation in join trees. *Int. J. Approx. Reason* **2000**, *15*, 1027–1059. [CrossRef]
12. Gómez-Olmedo, M.; Cano, A. Applying numerical trees to evaluate asymmetric decision problems. In *Symbolic and Quantitative Approaches to Reasoning with Uncertainty of Lecture Notes in Computer Science*; Nielsen, T., Zhang, N., Eds.; Springer: Berlin/Heidelberg, Germany, 2003; Volume 2711.
13. Salmerón, A.; Cano, A.; Moral, S. Importance sampling in Bayesian networks using probability trees. *Comput. Stat. Data Anal.* **2000**, *34*, 387–413. [CrossRef]
14. Cabañas, R.; Gómez-Olmedo, M.; Cano, A. Approximate inference in influence diagrams using binary trees. In Proceedings of the Sixth European Workshop on Probabilistic Graphical Models (PGM-12), Granada, Spain, 19–21 September 2012.
15. Cano, A.; Gómez-Olmedo, M.; Moral, S. Approximate inference in Bayesian networks using binary probability trees. *Int. J. Approx. Reason.* **2011**, *52*, 49–62. [CrossRef]
16. Gómez-Olmedo, M.; Cabañas, R.; Cano, A.; Moral, S.; Retamero, O.P. Value-Based Potentials: Exploiting Quantitative Information Regularity Patterns in Probabilistic Graphical Models. *Int. J. Intell. Syst.* **2021**, *36*, 6913–6943. [CrossRef]
17. Scutari, M. Learning Bayesian networks with the bnlearn R package. *J. Stat. Softw.* **2010**, *35*, 1–22. [CrossRef]
18. Scutari, M. Bayesian network constraint-based structure learning algorithms: Parallel and optimized implementations in the bnlearn R package. *J. Stat. Softw.* **2017**, *77*, 1–20. [CrossRef]
19. UAI 2014 Inference Competition. 2014. Available online: https://personal.utdallas.edu/~vibhav.gogate/uai14-competition/index.html (accessed on 15 June 2022).
20. UAI 2016 Inference Competition. 2016. Available online: https://personal.utdallas.edu/~vibhav.gogate/uai16-evaluation/index.html (accessed on 15 June 2022).
21. Kullback, S.; Leibler, R.A. On information and sufficiency. *Ann. Math. Stat.* **1951**, *22*, 76–86. [CrossRef]
22. Onisko, A. Probabilistic Causal Models in Medicine: Application to Diagnosis of Liver Disorders. Ph.D. Dissertation, Institute of Biocybernetics and Biomedical Engineering, Polish Academy of Science, Warsaw, March 2003.
23. Bobrowski, L. HEPAR: Computer system for diagnosis support and data analysis. In *Prace IBIB 31*; Institute of Biocybernetics and Biomedical Engineering, Polish Academy of Science: Warsaw, Poland, 1992.
24. Heckerman, D.; Horwitz, E.; Nathwani, B. Towards Normative Expert Systems: Part I. The Pathfinder Project. *Methods Inf. Med.* **1992**, *31*, 90–105. [CrossRef] [PubMed]
25. Andreassen, S.; Jensen, F.V.; Andersen, S.K.; Falck, B.; Kjærulff, U.; Woldbye, M.; Sørensen, A.R.; Rosenfalck, A.; Jensen, F. MUNIN—An Expert EMG Assistant. In *Computer-Aided Electromyography and Expert Systems*; Elsevier: Amsterdam, The Netherlands, 1989; Chapter 21.
26. Andreassen, S.; Hovorka, R.; Benn, J.; Olesen, K.G.; Carson, E.R. A Model-based Approach to Insulin Adjustment. In Proceedings of the 3rd Conference on Artificial Intelligence in Medicine, Vienna, Austria, 21–24 June 1991; pp.239–248.
27. Dechter, R. Bucket elimination: A unifying algorithm for Bayesian inference. *Artif. Intell.* **1997**, *93*, 1–27.
28. Shenoy, P.P.; Shafer, G.R. Axioms for probability and belief-function propagation. In *Uncertainty in Artificial Intelligence of Machine Intelligence and Pattern Recognition*; Shachter, R.D., Levitt, T.S., Kanal, L.N., Lemmer, J.F., Eds.; North-Holland: Amsterdam, The Netherlands, 1990; Volume 9.
29. Zhang, N.L.; Poole, D. Exploiting causal independences in Bayesian networks inference. *J. Artif. Intell. Res.* **1996**, *5*, 301–328. [CrossRef]